

Spectral Convergence of Mapped Chebyshev Methods

Bruno Costa ^{*} Wai-Sun Don [†] Aline Simas [‡]

November 17, 2003

Abstract

In this article we clarify some fundamental questions on the spectral convergence of a mapped Chebyshev method proposed by Kosloff and Tal-Ezer [14] and state approximations properties of general mappings of Chebyshev points. We develop a new technique based on the method of the stationary phase which provides a simple way to determine the spatial resolution power and spectral convergence of mapped Chebyshev methods. In particular, we prove a conjecture about the resolution power of the Tal-Ezer mapping, yielding, as a corollary, a rigorous and very simple demonstration that a minimum of π points per wavelength are needed in the original Chebyshev method, a well known fact which has been only heuristically demonstrated in the past literature.

1 Introduction

In the last decades spectral methods have become popular for the numerical solution of Partial Differential Equations (PDEs) due to their greater accuracy when compared to Finite Differences (FD) and Finite Elements (FE) methods with the same degree of freedoms. This happens because the rate of convergence of spectral approximations depends only on the smoothness of the solution, which is known in literature as "spectral accuracy". By contrast, in FD and FE, the order of accuracy is some fixed negative power of N , the number of grid points being used.

In spectral methods the solution is expressed as a finite expansion of some set of basis functions. When the PDE is written in terms of the coefficients of this expansion, the method is known as a Galerkin spectral method. Spectral collocation methods, also known as pseudospectral methods, is another subclass of spectral methods and are obtained when the test functions in the variational formulation are Dirac functions based on a pre-determined set of points, the collocation points. The resulting scheme approximates the derivatives by differentiating a global interpolant built through the collocation points. Spectral collocation methods deals with nonlinear terms more easily than Galerkin methods, for they are treated on a FD manner, via gridpoints values multiplication.

The set of collocation points is related to the set of basis functions as the nodes of quadrature formulae, which are used in the computation of the spectral coefficients from the grid values. For periodic problems the Fourier trigonometric basis is used and a related set of collocation points for the interval $[0, 2\pi]$ is given by the equispaced set

$$\theta_j = \frac{2\pi j}{N}, \quad j = 0, \dots, 2N - 1. \quad (1)$$

^{*}Departamento de Matemática Aplicada, IM-UFRJ, Caixa Postal 68530, Rio de Janeiro, RJ, C.E.P. 21945-970, Brazil. E-Mail: bcosta@labma.ufrj.br

[†]Brown University, Division of Applied Mathematics, Box F, 182 George Street, Providence, RI 02912, USA. E-Mail: wson@cfm.brown.edu

[‡]Departamento de Matemática Aplicada, IM-UFRJ, Caixa Postal 68530, Rio de Janeiro, RJ, C.E.P. 21945-970, Brazil. E-Mail: bcosta@labma.ufrj.br

In the nonperiodic case, Chebyshev polynomials are usually taken with their associated collocation points in the interval $[-1, 1]$ given by

$$y_j = \cos\left(\frac{\pi j}{N}\right), \quad j = 0, \dots, N. \quad (2)$$

The Fourier and Chebyshev basis shares the existence of a fast transform between physical and spectral spaces and this fact makes them the number one choice for periodic and nonperiodic problems, respectively. Without the FFT, a typical transform takes $O(N^{d+1})$ operations, where d is the spatial dimension. The FFT reduces this count to $O(N^d \log N)$. The transform between physical and spectral spaces is an essential step for computing derivatives, a process that takes only $O(N^d)$ operations in FD or FE.

On the other hand, the nonuniform distribution of the Chebyshev points leads to tight stability restrictions. For instance, for hyperbolic and parabolic equations, the time step restriction for explicit integration formulae is typically $\Delta t = O(N^{-2})$ and $\Delta t = O(N^{-4})$, respectively, while for FD and FE they are $\Delta t = O(N^{-1})$ and $\Delta t = O(N^{-2})$. The fact that the derivatives matrices are dense, makes implicit integration an expensive alternative.

The source of such restrictive time steps are credited to the agglomeration of the Chebyshev points near the boundaries, with a minimal grid spacing of order $\Delta x_{\min} = O(N^{-2})$, yielding a spectral radius of size $O(N^2)$ for the first derivative matrix (see [13, 16]). It is reasonable to argue that smaller grid spacing allows higher wavenumbers and, therefore, faster dynamics, requiring shorter time steps.

Kosloff and Tal-Ezer [14] have addressed this issue and proposed to map the Chebyshev points to a new set of collocation points with a greater minimal grid spacing in order to alleviate the time step restriction. The proposed mapping stretches the grid spacing on the boundary pushing the points to the center of the domain, generating a quasi-uniform grid. On their seminal work, they claimed that the mapping decreases the spectral radius of the derivative operator from $O(N^2)$ to $O(N)$, increasing the allowed time step from $O(N^{-2})$ to $O(N^{-1})$ for hyperbolic problems and from $O(N^{-4})$ to $O(N^{-2})$ for parabolic ones. The mapping is given by

$$x = g(y, \alpha) = \frac{\arcsin(\alpha y)}{\arcsin(\alpha)}, \quad (3)$$

and $\alpha \in (0, 1)$ is a parameter determining the strength of the endpoints separation. While many good properties arise from this new distribution of points, as a smaller roundoff error and a better resolution for higher modes, the map has branch-points singularities at $y = \pm \frac{1}{\alpha}$, introducing some approximation error. In [14], a way of choosing the parameter α in order to avoid the influence of these singularities in the numerical scheme was proposed and in [1], numerical results confirmed the effectiveness of the proposed numerical fix.

The new distribution of points given by the mapping (3) has distinct spatial resolution properties. In [14] a conjecture about the resolution power of the new set of points stated a bigger spatial resolution when compared to the Chebyshev points. However, only experimental results involving the decay of the spectral coefficients were shown. In [1], other numerical results along the same line corroborated the conjecture. In this work, we have gone deeper into the study of the decay of the spectral coefficients and through the analysis of the oscillatory integrals defining them, were able to come up with an analytical proof for the conjecture. The technique developed along with the proof provides a very simple test to measure the resolution power of general mappings of the Chebyshev points. Particularly, the test applied to the Chebyshev set itself confirms the well-known minimum of π points per wavelength, a fact which has been only indirectly demonstrated in the literature through the observance of the decay of spectral Bessel coefficients on a Chebyshev series (see [7]).

Another important issue related to the Kosloff-Tal-Ezer mapping is maintenance of the spectral convergence of the Chebyshev method. Some works reported loss of spectral convergence when using

the mapping (see [6, 11, 10]). All articles agree to the fact that "theoretical spectral convergence is lost, however, the mapped method is still useful for practical purposes". In our point of view, this has generated some confusion and denied credibility to the use of the mapping, which, on the other hand, has been praised by many authors due to its enhanced numerical properties (see [1, 4, 8]). These facts leads to the conclusion that the choice of the parameter α , which is crucial to the good functioning of the mapping, has not been understood in its entirety and deserves a more detailed discussion.

In [6], the convergence of the mapped method was analytically studied and interpolation error estimates have been obtained. However, the path taken on obtaining such estimates was too specific and fairly complicated, not making explicit which relevant properties of the mapping are determinant on its convergence behavior. Moreover, an estimate stating the lack of spectral convergence of the Kosloff-Tal-Ezer mapping was presented on a equivocated way, once again obscuring the role of the parameter α in the design of an effective mapped Chebyshev spectral method. In this work we discuss the spectral convergence (or the lack of it) of the Kosloff-Tal-Ezer mapping (3) and present a much simpler and more straightforward way to conclude on the spectral convergence of a general mapped Chebyshev method. Our approach does not involve the common Sobolev error estimates, but makes clear which aspects of the mapping are necessary for maintenance of the spectral convergence.

The article is divided as follows: In Section 2, we present the mapped method in more details and a discussion on the choice of the parameter α with regards to the results already known in literature. In Section 3, we prove the conjecture on the spatial resolution power of the mapped method. Section 4 contains the spectral convergence demonstration and, finally, in Section 5, we extend the theory to general mappings of Chebyshev points, applying the results to draw conclusions on the resolution power and spectral convergence of equidistant points and the original set of Chebyshev points.

2 Preliminaries and α -Spectral Convergence

New sets of collocation points generated through mappings of the Chebyshev points are important because they keep the possibility of using fast transforms. For instance, given a function $u(x)$ and a mapping $x = g(y)$, the derivative of $u(x)$ can be evaluated as

$$\frac{du}{dx} = \frac{du}{dy} \frac{dy}{dx}, \quad (4)$$

where $\frac{dy}{dx} = \frac{1}{g'(y)}$. At the grid points $x_j = g(y_j)$, (4) can be rewritten as

$$\vec{u}' = MD\vec{u}, \quad (5)$$

where M is the diagonal matrix with elements $M_{jj} = \frac{1}{g'(y_j)}$ and D is the classical Chebyshev differentiation matrix. Thus, \vec{u}' in (5) can be computed at an extra cost of only $O(N)$ operations, after the use of a FFT to compute $D\vec{u}$.

The mapping (3) stretches the Chebyshev points (2) close to the boundary by pushing the interior points towards the center of the interval $[-1, 1]$. This fact has two important consequences on the numerical properties of the mapped method. First, the maximum time step $\Delta t = O(\Delta x_{\min})$ is increased and, secondly, the maximum grid spacing Δx_{\max} is diminished, increasing resolution of the higher modes. These facts have been confirmed numerically in many works (see [1, 8, 14]).

Other important properties of the mapping (3) are:

- The mapping derivative $g'(y) = \frac{\alpha}{\arcsin(\alpha)} \frac{1}{\sqrt{1-(\alpha y)^2}}$ is singular at $y = \pm \frac{1}{\alpha}$;
- One can show [14] that

$$\begin{aligned} \Delta x_{\min} &\rightarrow \frac{2}{N} \quad \text{if } \alpha \rightarrow 1, \\ \Delta x_{\min} &\rightarrow 1 - \cos\left(\frac{\pi}{N}\right) \quad \text{if } \alpha \rightarrow 0. \end{aligned} \quad (6)$$

- If $\alpha = 1 - \frac{c}{N^2} + O(N^{-3})$, $c > 0$ then

$$\Delta x_{\min} = \frac{2}{\pi N} \left(\sqrt{\pi^2 + 2c} - \sqrt{2c} \right). \quad (7)$$

We see from (6) and (7) above that, indeed, the time step Δt can be increased from $\Delta t = O(N^{-2})$ to $\Delta t = O(N^{-1})$ as α increases from 0 to 1. However, the singularity of the mapping introduces an error ε on the computations, which can be controlled according to a polynomial approximation result in [9], which provides the following relation between α , N and ε :

$$\alpha = \operatorname{sech} \left(\frac{|\ln \varepsilon|}{N} \right). \quad (8)$$

From (8), we can infer a give and take relation between accuracy and resolution for a fixed grid with number of points N . Decreasing α , decreases the mapping error ε , increasing the overall accuracy. However, a smaller α means a larger Δx_{\max} at the center of the interval, sacrificing resolution for higher modes (see [14]). If the primary interest is accuracy, one should set ε as the machine error ε_M , avoiding in this way any influence of the mapping error in the computations.

In [8], it was pointed out that choosing $\varepsilon = \varepsilon_M$ might be too stringent and a better alternative is to set ε equal to the desired approximation error, leaving the global error unaffected, and allowing the use of a bigger Δt . In [8], a value of $\alpha = \cos(\frac{1}{2})$ enabled the use of a time step two times larger when applying the method to a multidomain simulation of the Maxwell's equations, with a value of ε about 10^{-7} (a single precision setting). Nevertheless, It should be noticed that this choice of α only resolves those modes to the given accuracy of $\varepsilon = 10^{-7}$ for the lower 2/3 Fourier spectrum while leaving the upper 1/3 Fourier spectrum unresolved. In effect, the increase of the time step Δt was obtained at the price of solving less than the optimal number of Fourier modes, for the given fixed grid. Furthermore, this might cause additional complications in the solution of PDEs which are non-linear in nature, since the generation of high unresolved modes demands an increase on the number of grid points, requiring filtering to damp the unresolved high modes. It is our opinion that the use of a smaller N , with the choice of $\varepsilon = \varepsilon_M$, is a wiser approach.

Remark 1 *Another interesting aspect of the mapping (3) is the choice of the arcsine function. We understand it as the optimal function to undo the agglomeration of the Chebyshev points caused by the cosine mapping of the equispaced set of points $\frac{j\pi}{N}$, $j = 0..N$, since one can see it as a out of phase arccosine function. The singularities comes from the infinite value of the derivative at the boundary points, which are needed to compensate the zero values of the cosine derivative and bring back the Chebyshev points close to an equispaced distribution. Other mappings with similar properties to the Tal-Ezer mapping can be tried (without singularities), and this is a subject of a work in progress.*

The spectral convergence of the mapped method has also been a controversial subject in the literature. The intrinsical dependence of the mapping on the parameter α has led to many mistaken analyses throughout the literature, since a bad choice for α may destroy any kind of convergence due to the contamination of the approximation error by the mapping error ε . In [14], two ways of choosing the parameter α were suggested, depending on what is given higher priority: accuracy or spatial resolution. If accuracy is desired, one must set α as before, in (8). On the other hand, one must choose

$$\alpha = \cos \left(\frac{j\pi}{N} \right), \quad (9)$$

if $\frac{N}{2} - j$ modes are to be resolved with the mapped method. Note that $\frac{N}{2}$ would be the maximum number of resolvable modes on an ideal equispaced grid, i.e., when $\alpha = 1$.

The first works reporting loss of spectral convergence (see [10, 11]) have used α as in (9), for small values of j , and showed numerical experiments where spectral convergence was not achieved.

Indeed, as pointed out in [8], substitution of such an α in (8) leads to $\lim_{N \rightarrow \infty} \varepsilon = e^{-j\pi}$, destroying any spectral accuracy.

In [6], the convergence of the mapped method has been analytically approached, using α as in (8). The following interpolation error estimative was obtained:

$$\|I^N u - u\| \leq \frac{C}{(1 - \alpha^2)^{\frac{m}{2} - \frac{3}{4}}} N^{-m} \|u\|_{H^m}, \quad (10)$$

where $I^N u$ is the interpolating function of u at $\{x_j\}_{j=0}^N$. The estimative above reduces to the classical result for the unmapped Chebyshev method in the case $\alpha = 0$ (see [3]).

Mere substitution of α as a function of N , as in (8), into (10) yields

$$\|I^N u - u\| \leq C N^{-\frac{3}{2}} \|u\|_{H^m}. \quad (11)$$

The above result was used in [6] to prove the loss of spectral convergence when using the mapped method. However, this is somewhat misleading, since choosing α as in (8) is advocated in order to bound the overall approximation error ε to a predetermined limit, which can be the machine precision. The constant C in (11) hides the relevant proportion of $|\ln \varepsilon|$ to the practical values of N being used. Choosing α as in (8) is, therefore, a practical procedure, specific to some particular experiment and must not be misunderstood as an analytic fix to the mapping.

It should be recalled that the mapping has singularities and, in practice, poor convergence will be attained once the error ε resulting from the singularities becomes relevant in the calculations. Thus, theoretical spectral convergence will never be achieved and one must not expect that, when conjugating a mapping with singularities to the Chebyshev spectral method. On the other hand, the mapping is still useful because, in practice, spectral convergence is effectively obtained, as confirmed by many experiments in [1] and by the good results obtained in [4], [8] and [11].

In the numerical experiments shown in [6], the value of ε in (8) was fixed at 10^{-16} , corresponding to a double precision arithmetics; however the computations were performed in quadruple precision, and this unfortunate combination led to a supposedly numerical confirmation of (11), since the mapped method slowed its convergence when the error reached 10^{-17} . This fact only confirms the usefulness of formula (8), as predicted by the approximation theory. In theory, ε is never going to be fixed, it should be decreased as the order of the approximation N increases.

For instance, substitution of the first two leading terms of the Taylor expansion of (8), that is, $\alpha \approx 1 - (\frac{|\ln \varepsilon|}{N})^2$, into (10) yields

$$\|I^N u - u\| \leq \frac{C}{(1 - \alpha^2)^{\frac{m}{2} - \frac{3}{4}}} N^{-m} \|u\|_{H^m} \approx C |\ln \varepsilon|^{-m + \frac{3}{2}} N^{-\frac{3}{2}} \|u\|_{H^m}. \quad (12)$$

By taking $|\ln \varepsilon| \approx N$, one will get an interpolation error of the form

$$\|I^N u - u\| \leq C N^{-m} \|u\|_{H^m}. \quad (13)$$

Thus, if ε is always taken as the machine error, it makes sense to say that the Kosloff-Tal-Ezer is spectrally accurate and the estimative (10) indeed corroborates this claim, since it does affirm that for a fixed value of α , convergence depends only on the smoothness of the function being approximated.

Due to the need of obtaining an estimative depending on the parameter α , the path chosen in [6] to arrive at (10) hides many of the relevant aspects of the mapping which are crucial to its unbounded convergence. In Section 4 below, we present a more straightforward and simpler proof of the spectral convergence of the mapped method, which makes explicit the important geometric and analytic aspects of the Kosloff-Tal-Ezer mapping.

3 Resolution Power of the Mapped Method

In this section we study the spatial resolution power of the mapped method by computing how many points per wavenumber are needed to represent a sinusoidal wave function as $\cos(mx)$ with the mapped set (3). We will use the stationary phase method to observe the rate of decay of the spectral coefficients and derive a relation between the number of collocation points and the maximum resolved wave number.

It is well known that on a uniformly spaced grid, the maximal resolved mode w_{\max} is the inverse of the grid spacing Δx . For instance, considering the equispaced Fourier grid (1), we have $\Delta x_{\max} = \frac{2}{N}$ and $w_{\max} = \frac{N}{2}$. In [7], trigonometric functions were expanded in Chebyshev polynomials, with the aid of the Bessel functions J_n , as

$$\sin(mx) = 2 \sum_{n=0}^{\infty} \frac{1}{c_n} J_n(m) \sin\left(\frac{1}{2}n\pi\right) T_n(x), \quad (14)$$

to observe that at least π polynomials per wavelength are needed to obtain a spectral rate of convergence for the series above. This is due to the fact that $J_n(m)$ goes to zero exponentially fast once n is larger than m and $\sin(mx)$ has $\frac{m}{\pi}$ wavelengths inside the interval $[-1, 1]$. Thus, although the Chebyshev grid (2) is nonuniform, $\Delta x_{\max} = \frac{\pi}{N}$ and we obtain $w_{\max} = \frac{1}{\Delta x_{\max}} = \frac{N}{\pi}$, confirming that resolution analysis is in straightforward relation with maximal spacing analysis.

What about the mapped Chebyshev method? As $\alpha \rightarrow 1$, the mapped Chebyshev grid becomes almost equally spaced and the Chebyshev polynomials become cosine functions with rational wavenumbers (see [14]). Therefore, one can infer that spatial resolution requires only 2 points per wavelength. A maximal spacing analysis reveals that the mapping (3) stretches the Chebyshev grid away from the boundary points, forcing Δx_{\max} to decrease and improving the overall spatial resolution. Since in the Chebyshev case, Δx_{\max} is found in the middle of the interval $[-1, 1]$, one can easily measure the maximum grid spacing of the modified method as $\Delta x_{\max}^g = g'(0, \alpha) \Delta x_{\max} = \frac{\pi}{N} \frac{\alpha}{\arcsin(\alpha)}$, yielding a maximum wave number $w_{\max}^g = \frac{N \arcsin(\alpha)}{\pi \alpha} > \frac{N}{\pi}$ for the mapped Chebyshev grid. Therefore, only $\pi \frac{\alpha}{\arcsin(\alpha)} (< \pi)$ points are needed per wavelength.

In Figure 1 below, we plot the interpolation error of the mapped method for the function $u(x) = \cos(mx)$ for several values of m and N . The horizontal axis is the ratio between the maximum wave number m_{\max}^g and the wavenumber $\frac{m}{\pi}$ given by

$$\frac{m_{\max}^g \pi}{m} = \frac{N \arcsin(\alpha)}{m \alpha} = \frac{N}{m g'(0, \alpha)}.$$

Note that spectral convergence starts only when this ratio exceeds 1, confirming the heuristic arguments above.

This result has been stated as a conjecture in [14] and it has been confirmed in later works through numerical experiments; a clear and analytical proof has never been shown (at least to the best of the authors' knowledge.) We provide such a proof in the following theorem, where a general technique providing a simple path for the computation of the spatial resolution power of mapped Chebyshev methods is developed.

Theorem 2 *The mapped method requires a minimum of $\frac{\pi \alpha}{\arcsin(\alpha)}$ points to start resolving the function $\cos(mx)$.*

Proof. The proof follows by considering Chebyshev expansion of $\cos(mx)$ as below:

$$\cos(mx) = \sum_{k=0}^{\infty} \hat{a}_k T_k(y),$$

where x is given by (3), and analyzing the decay of the spectral coefficients \hat{a}_k .

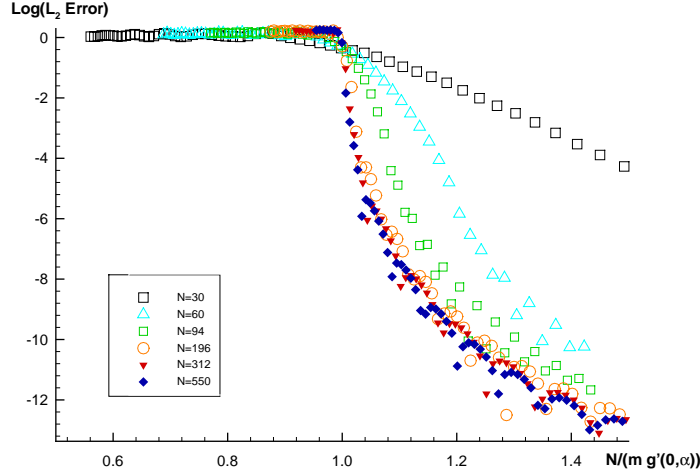


Figure 1: The normalized L_2 Error of the interpolating the function $\cos(mx)$ by the modified Chebyshev collocation methods for various wave number m and number of collocation grid N .

The Chebyshev coefficients above are given by

$$\hat{a}_k = \frac{2}{\pi} \int_{-1}^1 \frac{\cos(mx) T_k(y)}{\sqrt{1-y^2}} dy = \frac{2}{\pi} \int_0^\pi \cos(mg(\cos(\theta), \alpha)) \cos(k\theta) d\theta, \quad (15)$$

where $\theta = \arccos(y)$. If k is even (odd), $\cos(k\theta)$ is even (odd) with respect to $\theta = \frac{\pi}{2}$; $\cos(mg(\cos(\theta), \alpha))$ is even with respect to $\frac{\pi}{2}$. Therefore, (15) is equivalent to:

$$\hat{a}_k = \begin{cases} 0, & k \text{ odd,} \\ \frac{4}{\pi} \int_0^{\frac{\pi}{2}} \cos(mg(\cos(\theta), \alpha)) \cos(k\theta) d\theta, & k \text{ even.} \end{cases} \quad (16)$$

With the aid of the trigonometric identity $\cos(a) \cos(b) = \frac{1}{2}(\cos(a+b) + \cos(a-b))$ and $\cos(a) = \text{Re}\{\exp(ia)\}$, we may rewrite (16) as

$$\hat{a}_k = \frac{2}{\pi} \text{Re}\{H^+(\theta, k, m, \alpha) + H^-(\theta, k, m, \alpha)\}, \quad (17)$$

where

$$\begin{aligned} H^\pm(\theta, k, m, \alpha) &= \int_0^{\frac{\pi}{2}} \exp(i(mg(\cos(\theta), \alpha) \pm k\theta)) d\theta \\ &= \int_0^{\frac{\pi}{2}} \exp(ik(\beta g(\cos(\theta), \alpha) \pm \theta)) d\theta, \end{aligned} \quad (18)$$

and $\beta = \frac{m}{k}$ for $k = 1, \dots, \infty$. We will now show that convergence of H^\pm to zero as $k \rightarrow \infty$ is poor unless $k > \frac{m\alpha}{\arcsin(\alpha)}$.

We define

$$\Psi_\pm(\theta) = \beta g(\cos(\theta), \alpha) \pm \theta, \quad (19)$$

and by the Riemann–Lebesgue Lemma, $\Psi'_\pm(\theta) = \beta g'(\cos(\theta), \alpha) \pm 1$ cannot vanish in $[0, \frac{\pi}{2}]$, if one wants that \hat{a}_k goes to zero at least as k^{-1} . Thus, we need to verify for which values of θ , $\Psi'_\pm(\theta) \neq 0$ in $[0, \frac{\pi}{2}]$.

Since $g'(\cos(\theta), \alpha)$ is a decreasing function in $[0, \frac{\pi}{2}]$ given by:

$$g'(\cos(\theta), \alpha) = \frac{-\alpha}{\arcsin(\alpha)} \frac{\sin(\theta)}{\sqrt{1 - (\alpha \cos(\theta))^2}}, \quad (20)$$

with

$$g''(\cos(\theta), \alpha) = \frac{-\alpha(1 - \alpha^2)}{\arcsin(\alpha)} \frac{\cos(\theta)}{(1 - (\alpha \cos(\theta))^2)^{\frac{3}{2}}} \leq 0, \quad (21)$$

and $g'(\cos(0), \alpha) = 0$, $g'(\cos(\frac{\pi}{2}), \alpha) = \frac{-\alpha}{\arcsin(\alpha)} < 0$, for $\alpha \in (0, 1)$, we obtain $g'(\cos(\theta), \alpha) \in [\frac{-\alpha}{\arcsin(\alpha)}, 0]$.

Therefore $\Psi'_-(\theta) = \beta g'(\cos(\theta), \alpha) - 1 \leq -1 < 0$, for $\theta \in [0, \frac{\pi}{2}]$ and $\alpha \in (0, 1)$. $\Psi'_+(\theta)$ is bounded away from zero in $[0, \frac{\pi}{2}]$ iff $\beta |g'(\cos(\frac{\pi}{2}), \alpha)| < 1$, i.e., iff

$$k > mg'(0, \alpha) = m \frac{\alpha}{\arcsin(\alpha)}. \quad (22)$$

If $k = m \frac{\alpha}{\arcsin(\alpha)}$, then $\Psi'_+(\frac{\pi}{2}) = 0$ and by the stationary phase method (see [15]), the rate of convergence is given by the order of the first nonvanishing derivative of $\Psi_+(\theta)$ at the stationary point $\theta = \frac{\pi}{2}$. Since $\Psi''_+(\theta) = \beta g''(\cos(\theta), \alpha)$, we see from (21) and the expression for $\Psi'''_+(\theta)$ below:

$$\Psi'''_+(\theta) = \frac{m}{k} \left[\frac{-\alpha(1 - \alpha^2)}{\arcsin(\alpha)} \right] \left[-\sin \theta \left(1 - (\alpha \cos \theta)^2\right)^{-\frac{3}{2}} + \alpha \cos^2 \theta \sin \theta \left(1 - (\alpha \cos \theta)^2\right)^{-\frac{5}{2}} \right],$$

that \hat{a}_k goes to zero as $k^{-\frac{1}{3}}$, since $\Psi'_+(\frac{\pi}{2}) = \Psi''_+(\frac{\pi}{2}) = 0$ and $\Psi'''_+(\frac{\pi}{2}) \neq 0$.

Since truncation and interpolation errors are qualitatively similar (see [3]), the result above is the same as saying that $\pi \frac{\alpha}{\arcsin(\alpha)}$ points per wavenumber are needed for good spatial resolution with the Chebyshev spectral methods. ■

It is relevant to notice that the use of the auxiliary functions (18) and (19) in the demonstration above is not particular to the Kosloff–Tal-Ezer mapping. We will see in Section 6 below that the resolution power of other mappings can be studied in the same framework, in particular the classical case of the Chebyshev method itself.

We end this section pointing out that once the condition (22) is satisfied, $\Psi_{\pm}(\theta)$ are monotone functions in $[0, \pi]$ and their inverse functions are well defined. We will need this information in the study of spectral convergence of next section.

4 Spectral Convergence of the Kosloff–Tal-Ezer Mapping

We will now study the convergence of the Kosloff–Tal-Ezer method by looking to the rate of decay of the spectral coefficients (15). We rewrite the auxiliary functions $H^{\pm}(\theta, k, m, \alpha)$ in (24) as

$$\begin{aligned} H^{\pm}(\theta, k, m, \alpha) &= \int_0^{\frac{\pi}{2}} \exp(ik(\beta g(\cos(\theta), \alpha) \pm \theta)) d\theta \\ &= \int_0^{\frac{\pi}{2}} \exp[ik\Psi_{\pm}(\theta)] d\theta, \end{aligned} \quad (23)$$

and using the change of variables $\Psi_{\pm}(\theta) = y$ and its inverse function $\Psi_{\pm}^{-1}(y) = \theta$, we can rewrite the integrals above in a simpler form as:

$$H^{\pm} = \int_{\Psi_{\pm}(0)}^{\Psi_{\pm}(\frac{\pi}{2})} f_{\pm}(y) e^{iky} dy, \quad (24)$$

where

$$f_{\pm}(y) = \frac{1}{\Psi'_{\pm}(\Psi_{\pm}^{-1}(y))}. \quad (25)$$

Also,

$$\begin{aligned} \Psi_{\pm}\left(\frac{\pi}{2}\right) &= \beta \frac{\arcsin(\alpha \cos(\frac{\pi}{2}))}{\arcsin(\alpha)} \pm \frac{\pi}{2} = \pm \frac{\pi}{2}, \\ \Psi_{\pm}(0) &= \beta \frac{\arcsin(\alpha \cos(0))}{\arcsin(\alpha)} \pm 0 = \beta. \end{aligned}$$

We do not know the inverse function $\Psi_{\pm}^{-1}(y)$ explicitly, however, as we will see below, we only need to know their boundary values and symmetry properties. These will be used to compute the boundary values of $f_{\pm}(y)$ at $y = 0$ and $\frac{\pi}{2}$.

Integrating (24) by parts repeatedly, we obtain:

$$H^{\pm} = \sum_{l=0}^{M-1} \left\{ \left(\frac{1}{ik}\right)^{l+1} \left[f_{\pm}^{(l)}\left(\pm\frac{\pi}{2}\right) e^{\pm ik\frac{\pi}{2}} - f_{\pm}^{(l)}(\beta) e^{ik\beta} \right] \right\} - \left(\frac{1}{ik}\right)^M \int_{\beta}^{\pm\frac{\pi}{2}} f_{\pm}^{(M)}(y) e^{iky} dy$$

The integer superscript enclosed by parentheses denotes the order of the differentiation with respect to the variable y . Note that f_{+} and f_{-} are C^{∞} , since they are compositions of C^{∞} functions; the only obstacle to that would be $\Psi'_{\pm}(\theta)$ vanishing for some value of θ , but this cannot happen when the condition (22) is satisfied, as shown in Section 3.

From (16), we only need to check for k even, and from (17) the Chebyshev coefficient \hat{a}_k becomes

$$\hat{a}_k = \frac{\pi}{2} \operatorname{Re} \{ I_1 - I_2 - I_3 \},$$

where

$$\begin{aligned} I_1 &= \sum_{l=0}^{M-1} (ik)^{-(l+1)} (-1)^{\frac{k}{2}} \left(f_{+}^{(l)}\left(\frac{\pi}{2}\right) + f_{-}^{(l)}\left(-\frac{\pi}{2}\right) \right), \\ I_2 &= \sum_{l=0}^{M-1} (ik)^{-(l+1)} e^{ik\beta} \left(f_{+}^{(l)}(\beta) + f_{-}^{(l)}(\beta) \right), \\ I_3 &= (ik)^{-M} \left(\int_{\beta}^{\frac{\pi}{2}} f_{+}^{(M)}(y) e^{iky} dy + \int_{\beta}^{-\frac{\pi}{2}} f_{-}^{(M)}(y) e^{iky} dy \right). \end{aligned}$$

In order to obtain spectral convergence, we need to prove that the real parts of I_1 and I_2 vanish for any fixed integer $M \geq 1$ and $l = 0, \dots, M-1$, i.e., for the coefficients \hat{a}_k decay as k^{-M} , we need to show that

$$\begin{cases} f_{+}^{(l)}(\beta) + f_{-}^{(l)}(\beta) = 0 & \forall l, \\ f_{+}^{(l)}\left(\frac{\pi}{2}\right) + f_{-}^{(l)}\left(-\frac{\pi}{2}\right) = 0 & \forall l \text{ odd.} \end{cases} \quad (26)$$

The explicit expressions of the functions f_{\pm} in (25) are essential to obtain quantitative results of convergence, as it was done in [6], when error estimates depending on α were obtained. In this work, however, we are interested in the properties of f which are essential to spectral convergence and we will see below that they are determined by symmetry properties of the mapping function g . In Section 5, we present this as a generalization of the well-known result for the Chebyshev polynomials, whose spectral convergence is independent of the behavior of the function at the boundaries (see [7]).

We start the demonstration of (26) by establishing some properties of $\Psi_{\pm}(\theta)$ and its inverse function Ψ_{\pm}^{-1} , as stated in the following lemma:

Lemma 3 *If $k > \frac{m\alpha}{\arcsin(\alpha)}$, then $\Psi_+^{-1}(y) = -\Psi_-^{-1}(y)$ for $y \in [-\pi, \pi]$.*

Proof. It is easy to see from (19) that $\Psi_{\pm}(\theta)$ can be extended to $[-\pi, \pi]$ and since we are considering values of k satisfying (22), the results of last section guarantee that $\Psi_+(\theta)$ and $\Psi_-(\theta)$ are respectively increasing and decreasing functions in this interval. Therefore, $\Psi_+^{-1}(y)$ and $\Psi_-^{-1}(y)$ are well defined functions in $[-\pi, \pi]$.

Let $\tilde{g}(\theta) = g(\cos(\theta), \alpha)$, for a fixed α and note that from (3), \tilde{g} is an even function and is odd with respect to $\frac{\pi}{2}$. Thus, \tilde{g}' is an odd function which is even with respect to $\frac{\pi}{2}$. The proof follows easily from the definition of $\Psi_{\pm}^{-1}(y)$ and the fact that \tilde{g} is even. Note that $\Psi_{\pm}^{-1}(y)$ is the angle θ such that $\Psi_+(\theta) = y$, but $\Psi_+(\theta) = \beta\tilde{g}(\theta) + \theta = y$ and $\Psi_-(-\theta) = \beta\tilde{g}(-\theta) - (-\theta) = \beta\tilde{g}(\theta) + \theta = y$. Therefore, the angle θ , pre-image of y through Ψ_+ , is minus the pre-image of y through Ψ_- . ■

The first condition in (26) will be trivially satisfied once we prove the following result:

Theorem 4 $f_+(y) = -f_-(y)$ for $y \in [-\pi, \pi]$.

Proof. From the definitions of f_{\pm} in (25) we have:

$$\begin{aligned} f_+(y) &= \frac{1}{\Psi_+'(\Psi_+^{-1}(y))} = \frac{1}{\beta\tilde{g}'(\Psi_+^{-1}(y)) + 1} \\ &= \frac{1}{\beta\tilde{g}'(-\Psi_-^{-1}(y)) + 1} = \frac{1}{-\beta\tilde{g}'(\Psi_-^{-1}(y)) + 1} \\ &= \frac{-1}{\beta\tilde{g}'(\Psi_-^{-1}(y)) - 1} = \frac{-1}{\Psi_-''(\Psi_-^{-1}(y))} \\ &= -f_-(y). \end{aligned}$$

■

The way we will prove that $f_+^{(l)}(\frac{\pi}{2}) + f_-^{(l)}(-\frac{\pi}{2}) = 0$, for all l odd, is showing that each one of these terms is zero, as stated in the following theorem:

Theorem 5 $f_+^{(l)}(\frac{\pi}{2}) = f_-^{(l)}(-\frac{\pi}{2}) = 0$ for all odd l .

Proof. It is easily seen that $\Psi_+(\theta)$ changes concavity in $\frac{\pi}{2}$, since g changes concavity in $\frac{\pi}{2}$. More than that, g is odd with respect to $\frac{\pi}{2}$, therefore all its even derivatives vanish at $\frac{\pi}{2}$. This clearly implies that the even derivatives of $\Psi_+(\theta)$ also vanish there. Moreover, $\Psi_+''(\theta)$ is an odd function with respect to $\frac{\pi}{2}$:

$$\Psi_+''(\theta) = \beta g''(\cos(\frac{\pi}{2}), \alpha) = \frac{m - \alpha(1 - \alpha^2)}{k \arcsin(\alpha)} \frac{\cos(\theta)}{(1 - (\alpha \cos(\theta))^2)^{\frac{3}{2}}}.$$

Since all even derivatives of $\Psi_+(\theta)$ change concavity at $\frac{\pi}{2}$, the same happens to $\Psi_+^{-1}(y)$ at $y = \Psi_+(\frac{\pi}{2}) = \frac{\pi}{2}$. This implies that $(\Psi_+^{-1})^{(l)}(\frac{\pi}{2}) = 0$, for l even. Thus, $f_+^{(l)}(\frac{\pi}{2}) = 0$, for l odd. Finally, $\Psi_-(y)$ has the same behavior at $-\frac{\pi}{2}$ and analogous results are obtained for $\Psi_-^{-1}(y)$ at $y = \Psi_-(-\frac{\pi}{2}) = -\frac{\pi}{2}$, which are $(\Psi_-^{-1})^{(l)}(-\frac{\pi}{2}) = 0$, for l even and $f_-^{(l)}(-\frac{\pi}{2}) = 0$, for l odd. ■

5 General Mappings

It is easy to notice in the proofs above that only few properties of the mapping $g(y, \alpha)$ are necessary to validate the theorems of last section. Clearly, the Kosloff–Tal–Ezer mapping is not unique at increasing the overall resolution and still maintaining spectral convergence. In this section, we discuss which properties of general mappings of the Chebyshev points are necessary to obtain the same numerical improvements as the Kosloff–Tal–Ezer mapping.

In the results of last sections, we have implicitly defined that resolution was attained when a significant jump in the decay rate of the coefficients was observed, or when at least a decay of order $O(k^{-1})$ was achieved. Only after this we looked for spectral convergence, meaning that the vanishing of all boundary terms in the systematic integration by parts had to be obtained. We now discuss the roles of conditions (22) and (26) in the general two-stage process described above.

We start by noticing that the mapping $\tilde{g}(\theta) = g(\cos(\theta), \alpha)$ can be looked as a mapping from the equispaced set of points $\{\theta_j\} \subset [0, \pi]$ to the interval $[-1, 1]$ rather than a mapping from the Chebyshev points. Also, \tilde{g} will be restricted to be odd with respect to $\frac{\pi}{2}$, i.e., only symmetric distributions of points with respect to the center of the interval $[-1, 1]$ will be considered. This property of \tilde{g} keeps the definitions of the coefficients \hat{a}_k 's as in (16) and (17) unaltered and everything is the same up to the definition of the auxiliary functions $\Psi_{\pm}(\theta) = \beta\tilde{g}(\theta) \pm \theta$. It is now clear to see that spatial resolution will depend on $\|\tilde{g}'\|_{\infty}$. This is the quantity which controls the minimal value of k in the ratio $\beta = \frac{m}{k}$ in order to $\Psi_{\pm}(\theta)$ to inherit the strict monotonicity of the linear term $\pm\theta$, which is necessary for the nonexistence of stationary points and the consequential $O(k^{-1})$ rate of decay.

For instance, if we look to the classical cases of an equispaced distribution and the Chebyshev set itself, respectively given by the mappings

$$g_e = 1 - \frac{2\theta}{\pi} \quad (27)$$

and

$$g_c = \cos(\theta), \quad (28)$$

we easily obtain that $\frac{m}{k}\|\tilde{g}'\|_{\infty} \pm 1 \neq 0$ if

$$k > \frac{2m}{\pi} = 2N \quad \text{if} \quad \tilde{g}_x = g_e \quad (29)$$

and

$$k > m = N\pi \quad \text{if} \quad \tilde{g}_x = g_c. \quad (30)$$

It is very interesting to notice that the Chebyshev resolution condition (30) has been only heuristically demonstrated in the past literature, through the observance of the Chebyshev series with Bessel coefficients in (14) above, although in [13], the sufficiency side of this condition has been shown, i.e., that π points per wavelength is enough for resolution. More interesting yet is to observe the sharpness of the results provided by this technique. As noticed in [12], if $k = N\pi$, equation (9.1.61) in [2] yields:

$$0 < J_k(k) < \frac{\sqrt{2}}{3^{2/3}\Gamma(2/3)k^{1/3}},$$

showing that (30) is strict. This same result is also analytically obtained through the auxiliary functions $\Psi_{c\pm} = \beta\tilde{g}_c \pm \theta$, analogously as in the demonstration of Theorem 1, by noticing that $\Psi_{c+}'(\frac{\pi}{2}) = \Psi_{c+}''(\frac{\pi}{2}) = 0$ and $\Psi_{c+}'''(\frac{\pi}{2}) \neq 0!!!$

The study of spectral convergence is intimately connected to a deeper understanding of the meaning of conditions (26) above. The first condition in (26) is guaranteed by the evenness of the differentiable extension of the mapping \tilde{g} . Lemma 1 and Theorem 2 are consequences of this property, whose existence is guaranteed, in its turn, by the zero derivative of \tilde{g} at $\theta = 0$. The Chebyshev mapping (28) itself has a differentiable even extension and obviously satisfies the first condition in (26), since it is spectrally convergent. On the other hand, the equispaced mapping (27) does not satisfy the evenness condition in (26) and, therefore, interrupts the integration by parts process, not achieving spectral convergence, as it is well-known. Thus, the Kosloff-Tal-Ezer mapping is only one of a class of mappings which automatically satisfy the evenness condition: mappings of the form:

$$\tilde{g}(\theta) = g(\cos\theta). \quad (31)$$

It is not hard to associate the evenness condition above with the singular status of the Sturm–Liouville problem

$$(p'(x) \phi_k(x))' = -\lambda_k \omega(x) \phi_k(x),$$

which is guaranteed by the vanishing of $p(x)$ at the boundaries (see [3]). For instance, given the mapping $x = g(y)$, with inverse $y = h(x)$, we define the mapped Chebyshev eigenfunctions $Q_k(x) = T_k(h(x))$, which are solutions to the modified Sturm–Liouville problem

$$(p'_g(x) Q_k(x))' = -k^2 \omega_g(x) Q_k(x) \quad (32)$$

where $\omega_g(x) = \omega_c(y) \frac{dh}{dx}$, $\omega_c(y) = \frac{1}{\sqrt{1-y^2}}$ is the original Chebyshev weight function, and

$$p_g(x) = \frac{1}{\omega_g(x)} = \frac{1}{\omega_c(y) \frac{dh}{dx}} = \frac{\sqrt{1-h^2(x)}}{\frac{dh}{dx}}.$$

Thus, if $h(\pm 1) = \pm 1$, i.e., h keeps the endpoints fixed, then problem (32) is a singular Sturm–Liouville problem once h is "well-behaved" in the sense of satisfying conditions (22) and (26) of last section.

The second condition in (26) is satisfied once the mapping \tilde{g} changes concavity at $\theta = \frac{\pi}{2}$. This is also automatically satisfied by mappings of the type (31) above. On the other hand, the equispaced mapping (27) does not satisfy this condition either. It is relevant to observe that we are ultimately considering the expansion of the function $\cos(m\tilde{g}(\theta))$ on a cosine series, as can easily be seen in Theorem 1. Therefore, evenness and change of concavity at $\frac{\pi}{2}$ are reasonable conditions to ask of a (symmetric) mapping to maintain the spectral convergence of the Chebyshev points.

The results of Lemma 4 and Theorems 5 and 6 are easier understood if we look to Figure 2 below, where we draw the graph of a typical mapping \tilde{g} and its related auxiliary functions Ψ_{\pm} , together with their inverse functions Ψ_{\pm}^{-1} . For instance, it is direct to check the validity of Theorem 5 and also to observe the change of concavity of Ψ_{\pm} and Ψ_{\pm}^{-1} , necessary for the demonstration of Theorem 6.

6 Conclusions

In this work we discussed two relevant aspects of the Kosloff–Tal–Ezer mapping of the Chebyshev points: Its resolution power and spectral convergence. Through the use of the Stationary Phase Method we demonstrated its increased spatial resolution with respect to the classical Chebyshev method and proved its spectral convergence for a fixed α , clarifying some questions on the spectral convergence of the Kosloff–Tal–Ezer method, which has been a controversial subject in the literature.

The techniques here developed showed to be useful for the analysis of general mappings. In particular, we were able to demonstrate the classical result on the resolution power of the Chebyshev polynomials, which had only been heuristically demonstrated in the literature. The results are also of great use in the designing of new mappings with better resolution properties. For instance, they provide a deep enough understanding to consider a modification of the Kosloff–Tal–Ezer mapping with a variable parameter α . Patching of mappings can also be considered in the same framework. Perhaps, a modification of the Tal–Ezer mapping will provides us an spectral method with a true $O(N^{-1})$ time step. These are subjects of a forthcoming work.

7 Acknowledgments

Part of the research was done during the visit of the second author to the Departamento de Matemática Aplicada, IM-UFRJ. The first author was partly supported by CNPQ, grant number 300315/98-8. The research of the second author was partly supported by the DOE grant number DE-FG02-96ER25346.

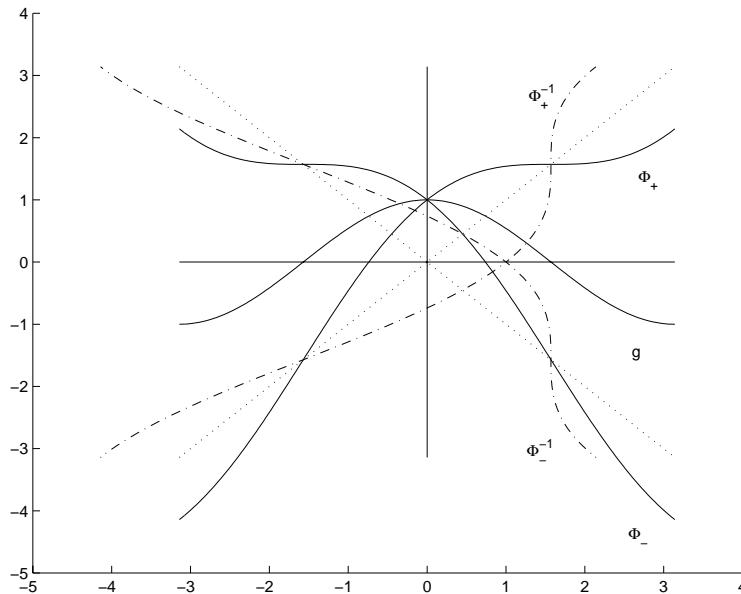


Figure 2: A typical mapping \tilde{g} and its related auxiliary functions Ψ_{\pm} , together with their inverse functions Ψ_{\pm}^{-1}

References

- [1] W. S. Don and A. Solomonoff, *Accuracy Enhancement for Higher Derivatives Using Chebyshev Collocation and a Mapping Technique*, SIAM J. Sci. Comput., Vol. 18, (1997) pp. 1040-1055.
- [2] M. Abramowitz and I. A. Stegun, *Handbook of Mathematical Functions*, Dover, New York, 1972.
- [3] C. Canuto, M. Y. Hussaini, A. Quarteroni and T. A. Zang, *Spectral Methods in Fluid Dynamics*, Springer Series in Computational Physics, Springer, Berlin, 1988.
- [4] J. M. Carcione, *A 2D Chebyshev Differential Operator for the Elastic Wave Equation*, Comput. Meth. Appl. Mech. Engr., Vol. 130, (1996), pp. 33-45.
- [5] B. Costa and W. S. Don, *On the Computation of Higher Order Pseudospectral Derivatives*, Appl. Numer. Math., Vol. 33, No. 1, (2000), pp. 151-159.
- [6] M. R. Abril-Raimundo and B. García-Archilla, *Approximation properties of a mapped Chebyshev method*, Appl. Numer. Math., Vol. 32, (2000) pp. 119-136.
- [7] D. Gottlieb, S. A. Orszag, *Numerical Analysis of Spectral Methods: Theory and Applications*, SIAM, Philadelphia, PA, 1977.
- [8] J. S. Hesthaven, P. G. Dinesen and J. P. Lynov, *Spectral Collocation Time-Domain Modeling of Diffractive Optical Elements*, J. Comput. Phys., Vol. 155, (1999), pp. 287-306.
- [9] A. I. Markushevich, *Theory of Functions of a Complex Variable*, Chelsea, New York (1977).
- [10] S. C. Reddy, J. A. C. Weideman and G. F. Norris, *On a Modified Chebyshev Pseudospectral Method*, (unpublished, Oregon State University, Corvallis, OR).

- [11] R. A. Renaut and Y. Su, *Evaluation of Chebyshev Pseudospectral Methods for Third Order Differential Equations*, Numer. Algo., Vol. 16, No. 3, (1997), pp. 255-281.
- [12] J. L. Mead and R. A. Renaut, *Accuracy, Resolution and Stability Properties of a Modified Chebyshev Method*, SIAM J. Sci. Comput., Vol. 24, No. 1, (2002), pp. 143-160.
- [13] J. A. C. Weideman and L. N. Trefethen, *The Eigenvalues of Second-Order Spectral Differentiation Matrices*, SIAM J. Numer. Anal., Vol. 23, No. 6, (1988)
- [14] D. Kosloff and H. Tal-Ezer, *Modified Chebyshev Pseudospectral Method With $O(N^{-1})$ Time Step Restriction*, J. Comput. Phys., Vol. 104, (1993), pp. 457-469.
- [15] C. M. Bender and S. A. Orszag, *Advanced Mathematical Methods for Scientists and Engineers*, McGraw Hill Book, New York (1978)
- [16] L. N. Trefethen and M. R. Trummer, *An Instability Phenomenon in Spectral Methods*, SIAM J. Numer. Anal., Vol. 24, No. 5, (1987)